

THE CRAB NEBULA. I. SPECTROPHOTOMETRY OF THE FILAMENTS

ROBERT A. FESEN¹ AND ROBERT P. KIRSHNER²

Department of Astronomy, University of Michigan

Received 1981 September 1; accepted 1981 December 14

ABSTRACT

New spectrophotometry for ten positions in the Crab Nebula is presented which provides relative line intensities for the wavelength region 3700 to 7400 Å. Electron temperatures determined from [O III] line intensities range from 11,000 to 18,300 K, with generally lower temperatures indicated from the lines of [O II], [N II], and [S II]. Electron densities estimated from the ratio of the [S II] $\lambda\lambda 6717, 6731$ lines range from 550 to 3500 cm⁻³ with a typical value of 1300 cm⁻³ for the filaments measured. The Balmer decrement for many filaments is consistent with pure recombination, but a few filaments exhibit slightly steeper decrements. Helium line intensities vary considerably among filaments with a few northern filaments showing He I $\lambda 5876$ line emission that is weaker by a factor of 3. Several faint emission features are measured and identified; in particular, we confirm the presence of a moderately strong line at $\lambda 7378$ which may be due to [Ni II]. A wide range of ionization states is present within some filaments as demonstrated by lines of [Fe II], [Fe III], [Fe V], and [Fe VII].

Subject headings: nebulae: Crab Nebula — nebulae: supernova remnants — spectrophotometry

I. INTRODUCTION

The Crab Nebula has two distinct types of emission: the amorphous region emits a continuous spectrum, and the nebula's filaments produce an emission-line spectrum. Because of the distinct likelihood that the filaments represent largely uncontaminated debris from the original supernova star, the emission line properties of the filaments deserve thorough investigation. In this paper we present new measurements of ten positions in the filaments.

Optically, the Crab's filaments show emission lines of He I, He II, [N II], [S II], [O I], [O II], and [O III], and relatively faint hydrogen lines (Minkowski 1942). Woltjer (1958), in an extensive study of the Crab, tentatively concluded that helium was overabundant relative to the solar value and might account for a significant fraction of the total mass of the filaments. He estimated the filaments had an [O III] electron temperature of about 17,000 K with an average electron density of around 1500 cm⁻³. His rather crude density estimates were consistent with the electron density range of 500 to 3700 cm⁻³ estimated by Osterbrock (1957) using [O II] line strengths. Recent high quality spectrophotometric studies by Miller (1978) and Davidson (1978, 1979) have not only confirmed the high helium abundance, but they have also permitted a more complete examination of the filaments' abundances and physical conditions.

Despite these investigations, additional spectroscopic data on the filaments are useful. Only a fraction of the Crab filaments have been accurately measured spectroscopically, and additional observations are required to

ensure a representative sampling of the filaments' emission properties. While the overall continuum and line flux has been measured by Kirshner (1974) and Davidson, Crane, and Chincarini (1974), substantial spectral line variations among filaments have been observed by Woltjer (1958), Trimble (1970), and Davidson (1978, 1979). Also, parameters such as the range of electron temperatures and densities as well as the Balmer decrement have not been thoroughly investigated. Improving the estimate for a typical filament's density will help provide a firmer estimate for the nebula's total mass.

This paper reports on new spectroscopic observations of the Crab Nebula's filaments and also on some physical properties that can be deduced directly from the data. Detailed spectral line modeling and interpretation is treated in a companion work (Henry and MacAlpine 1982, hereafter Paper II).

II. OBSERVATIONS

We present spectrophotometric data taken at ten separate locations in the Crab Nebula's filaments. The regions were selected based upon their brightness and spectral properties as determined from Miller's (1974) color photograph and Chevalier and Gull's (1975) interference filter photographs. Filament selection was also made to limit the severity of emission line overlap from adjacent or superimposed filaments. The observations were obtained with a 2000 channel intensified Reticon spectrometer attached to the 1.3 m telescope of the McGraw-Hill Observatory at Kitt Peak. The spectrometer is a pulse counting system employing six stages of image intensification, and a self-scanned diode array connected to pulse counting and event centering electronics that produces a digital spectrum. Using a 300 l mm⁻¹ grating, this instrument has a spectral

¹ NAS-NRC Postdoctoral Research Associate, NASA Goddard Space Flight Center.

² Alfred P. Sloan Foundation Research Fellow.

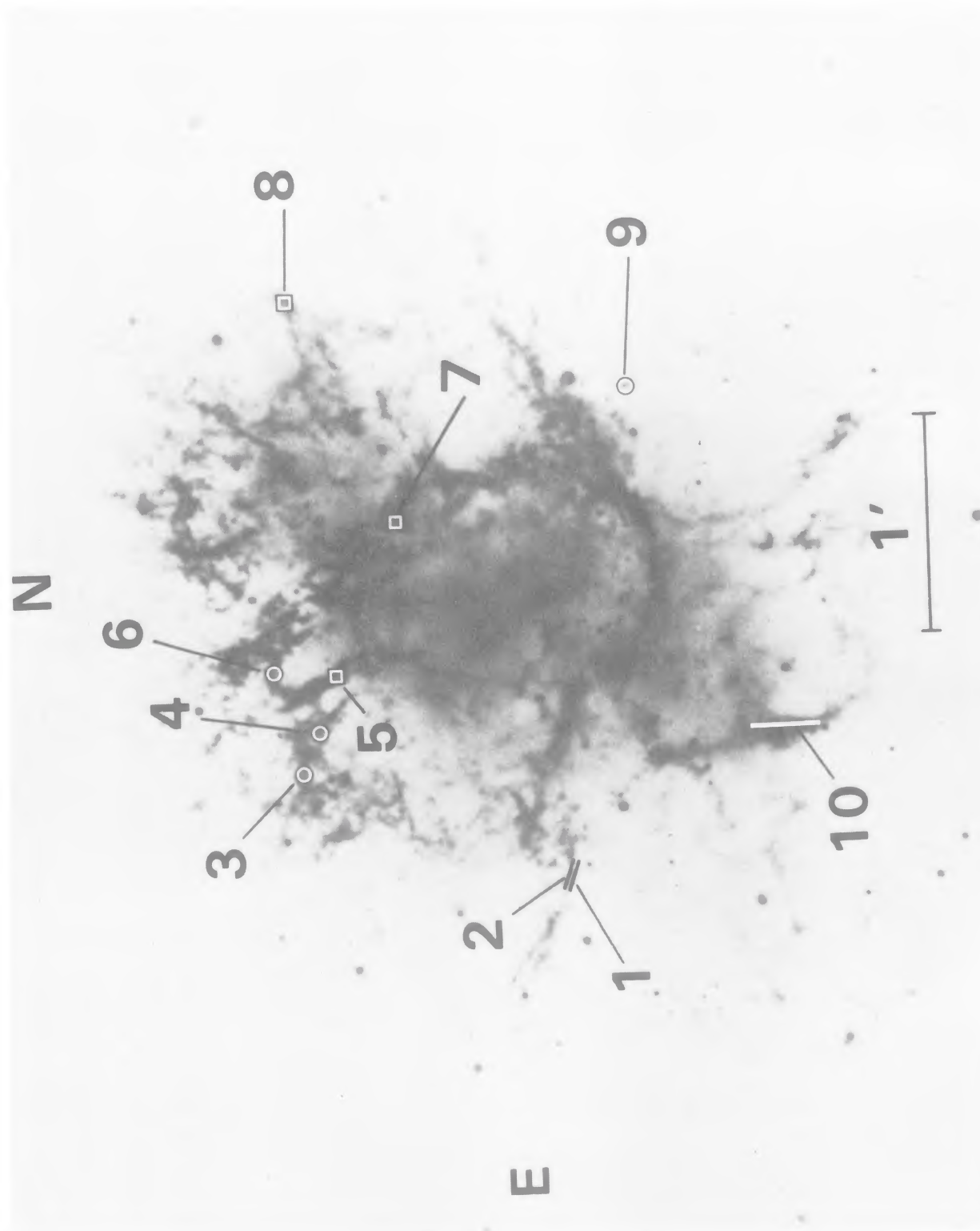


FIG. 1.—Reproduction of Baade's broad-band red photograph of the Crab Nebula showing the slit locations for the ten regions studied

SPECTROPHOTOMETRY OF CRAB FILAMENTS

3

TABLE 1
LOCATIONS OF SLIT POSITIONS

Position Number	Location Relative to the Pulsar
1	73°E 4"S
2	72 E 1 S
3	45 E 72 N
4	26 E 65 N
5	16 E 63 N
6	10 E 77 N
7	29 W 45 N
8	89 W 74 N
9	67 W 18 S
10	29 E 60 S

coverage of about 3500 Å with a resolution of 7 Å (FWHM).

The slit positions are listed in Table 1 and shown in Figure 1. Aperture positioning was accomplished using a television guiding system that generally held setting errors to less than 2". Integration times, slit sizes, spectral coverage, and resolution for each position are given in Table 2. Sky measurements with equal integration times were made alternately with the object scans about every 10 minutes and were taken at locations well outside the nebula. Data reduction consisted of correcting for detector dead time, subtracting sky scans, placing the data on a linear wavelength scale, and correcting for atmospheric extinction using average Kitt Peak extinction values. Flux calibrations for each night were obtained through observations of two or three white dwarfs (Oke 1974; Stone 1977).

A line measuring and deblending computer program using smoothed Gaussian line profiles constructed from object emission lines was used to deblend overlapping

line profiles and to obtain relative line intensities. The observed line intensities, $F(\lambda)$, together with the line intensities corrected for interstellar reddening, $I(\lambda)$, assuming $E(B-V) = 0.5$ (Miller 1973; Wu 1981) are listed in Table 3. The values are given relative to $H\beta$ where $F(H\beta) = 100$ except for position 7', where $I(H\alpha) = 300$ since $H\beta$ could not be accurately measured. At many slit positions, fainter sets of emission lines were observed due to neighboring or superposed filaments. The relative line intensities of these secondary emission features were measured when they had a sufficiently different radial velocity to permit reasonably accurate deblending from the brighter filaments' emission and are indicated in Table 3 by primed position numbers. The scans for all positions except 9 are shown in Figures 2 and 3.

The accuracy of the line intensity measurements reflects the line's photon statistics, the flux calibration from standard stars, and emission line deblending. The relative strengths for position 3 and the faint filament emission lines seen at positions 5, 7, and 8 (i.e., 5', 7', and 8') are the most uncertain due simply to poor photon statistics. Flux calibration errors were estimated by comparing the relative flux calibration of the individual standard stars. Comparisons indicate that such errors are 15% or less for every night. The accuracy of our line measurements where serious blending was not a problem was determined from emission lines whose relative strengths are known (e.g., [O III] $\lambda\lambda 4959, 5007$). We estimate the relative line strengths given in Table 3 are accurate to better than 20% for the strongest lines where $F(\lambda) \geq 200$, 20%-30% for lines whose $F(\lambda)$ is between 50 and 200, and 30%-50% for the fainter lines where $F(\lambda) \leq 50$. Larger uncertainties exist for lines near the very ends of the spectrum (e.g., [O II], $\lambda\lambda 3727$ and $\lambda 7325$) and for lines whose profiles were badly blended with

TABLE 2
JOURNAL OF OBSERVATIONS

UT Date	Slit Position	Integration Time (s)	Slit Size	Spectral Coverage (Å)	Resolution FWHM (Å)
1977 Dec 5	5	3000	3" × 5"	3700-7400	7
1977 Dec 6	1	3000	2" × 10"	3700-7400	7
1977 Dec 6	7	2500	3" × 5"	3700-7400	7
1977 Dec 7	2	1000	2" × 10"	3700-7400	7
1977 Dec 7	7	2500	3" × 5"	3700-7400	7
1977 Dec 8	8	4800	3" × 5"	3700-7400	7
1977 Dec 9	6	1000	3" cir.	3700-7400	7
1977 Dec 9	3	300	3" cir.	3700-7400	7
1977 Dec 9	4	4000	3" cir.	3700-7400	7
1977 Dec 10	8	2500	3" × 5"	6400-7600	4
1977 Dec 11	8	6000	3" × 5"	6400-7600	4
1977 Dec 17	4	2900	3" cir.	3600-4300	2
1979 Jan 1	9	5100	5'6 cir.	3600-5250	5
1980 Nov 12	10	2400	4" × 20"	3700-7400	12
1981 Feb 24	10	4200	3" × 20"	6000-7500	5
1981 Feb 25	6	3600	3" × 20"	6000-7500	5
1981 Feb 25	^a	1800	3" × 40"	6000-7500	5

^a Approximately Miller's 1978 position 2.

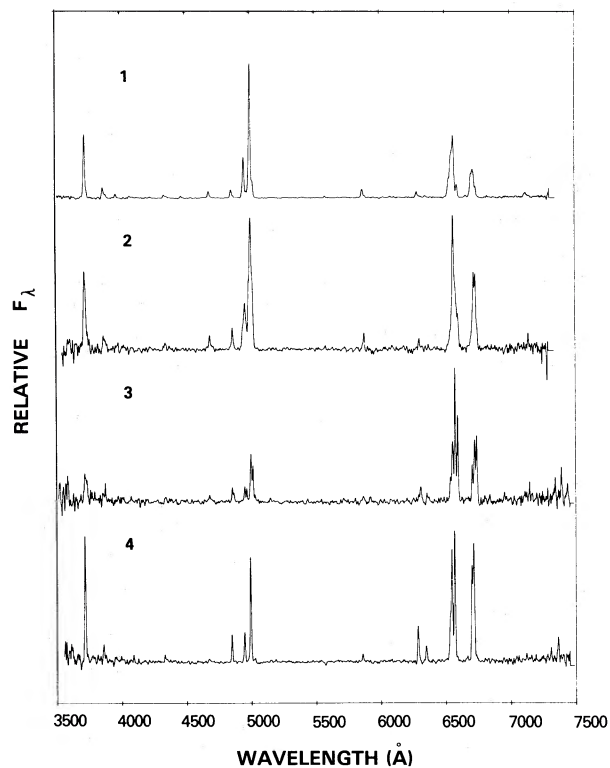


FIG. 2a

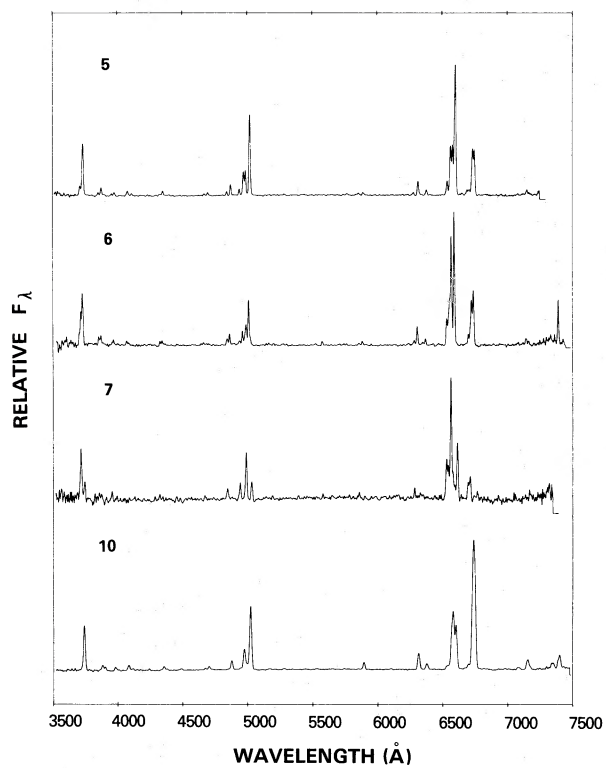


FIG. 2b

FIG. 2.—Spectrophotometric scans for eight regions in the Crab Nebula's filaments. Relative flux per unit wavelength is plotted vs. observed wavelength. The resolution of the data as shown is approximately 10 Å.

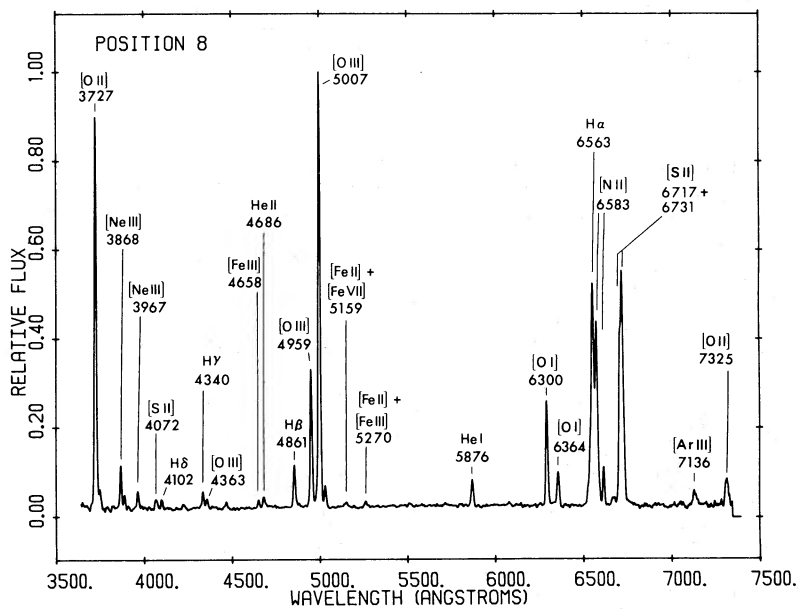


FIG. 3.—Spectrophotometric scan for position 8. Relative flux per unit wavelength is plotted vs. observed wavelength. Laboratory wavelength identifications are indicated for most of the measured emission features.

SPECTROPHOTOMETRY OF CRAB FILAMENTS

5

TABLE 3
RELATIVE LINE INTENSITIES
($I_{H\beta} = 100$; $E_{B-V} = 0.5$)

LINE	$\lambda(\text{\AA})$	FILAMENT POSITIONS									
		1		2		3		4		5	
		$F(\lambda)$	$I(\lambda)$	$F(\lambda)$	$I(\lambda)$	$F(\lambda)$	$I(\lambda)$	$F(\lambda)$	$I(\lambda)$	$F(\lambda)$	$I(\lambda)$
[O II].....	3727	756	1200	(356)	(564)	(220)	(349)	464	736	582	922
[Ne III].....	3869	125	187	51	76	57	85	69	104
He I + H ζ	3889	(45)	(69)	15	22
[Ne III] + He.....	3968	47	68	31	45
[S II].....	4071	(22)	(31)	36	51
H δ	4102	(21)	(28)	18	25
[Fe V].....	4227
H γ	4340	38	48	37	47	25	32	39	49
[O III].....	4363	20	26	<20	<26
He I.....	4471	20	24
[Fe III].....	4658	17	18
He II.....	4686	82	88	75	81	(51)	(55)	13	14	28	30
H β	4861	100	100	100	100	100	100	100	100	100	100
[O III].....	4959	482	463	215	206	111	107	113	109	191	184
[O III].....	5007	1600	1510	634	597	365	344	386	364	679	640
[Fe II] + [Fe VII].....	5159	8	7
[N I].....	5199	<15	<13	9	8	<12	<11
[Fe II] + [Fe III].....	5270	10	9
[N II].....	5755	<15	<11	<10	<7	14	10
He I.....	5876	110	77	80	56	(40)	(28)	29	20	24	17
[Fe VII].....	6087	(7)	(5)
[O I].....	6300	72	45	(43)	(27)	(110)	(67)	152	95	119	75
[S III].....	6312	<13	<8
[O I].....	6364	20	12	71	43	46	28
[N II].....	6548	210	124	(47)	(28)	181	106	168	99	396	233
H α	6563	550	322	556	324	(510)	(299)	433	254	423	249
[N II].....	6583	650	379	140	82	(555)	(324)	517	302	1190	695
He I.....	6678	21	12	15	8
[S II].....	6717	251	142	320	181	261	148	373	211	386	218
[S II].....	6731	(305)	(172)	300	169	(300)	(169)	473	267	371	210
[Ar III].....	7136	(58)	(30)	117	61	45	23
[Fe II].....	7155
[O II].....	7325	(34)	(17)
$f(H\beta)$ ergs cm $^{-2}$ s $^{-1}$		1.7 E-14		1.8 E-1Y		8.5 E-15		5.5 E-15		2.2 E-14	

neighboring lines or with other filament emission features, as was often the case with the H α and [N II] lines. Line intensities with larger uncertainties than those listed above are indicated in Table 3 by parentheses. Errors in listed absolute H β fluxes can be as much as 50%. We note that Davidson's (1979) and our data for the same filament (our position 8; his D1) are in good agreement within stated errors.

A few higher dispersion scans covering the wavelength region 6300–7600 Å were also obtained at positions 6, 8, 10, and Miller's position 2. These data were taken principally to investigate the strength of the suspected [Ni II] line at 7378 Å. Because these scans contained some second order overlap, they were not used to estimate relative fluxes. However, the data (see Fig. 4) are useful for studying the presence and approximate relative strengths of faint emission features in the 6800–7500 Å region.

The Crab Nebula's filaments are not particularly easy to observe spectroscopically due to their large radial velocities (up to = +1500 km s $^{-1}$) and the small spatial scale on which significant emission line variations can occur. As reported by Munch (1958), considerable fluctuations in radial velocity can be present along the line of sight often resulting in the blending of emission features. The morphology of at least some filaments as discontinuous clumps on a small spatial scale (Baade 1942; Trimble 1970) can lead to dramatic and abrupt line strength changes when the slit is shifted by just a few arcsec making it difficult to sample the line emission from just a single region. It is this small scale filamentary structure which makes it important to reposition the slit accurately during the observations. Also, some of the filaments are not particularly bright which, for filaments lying within or superposed on the amorphous regions, can lead to significantly lower signal-to-noise ratio levels.

TABLE 3—Continued

LINE	$\lambda(\text{\AA})$	FILAMENT POSITIONS									
		5'		6		7		7'		8	
		$F(\lambda)$	$I(\lambda)$	$F(\lambda)$	$I(\lambda)$	$F(\lambda)$	$I(\lambda)$	$F(\lambda)$	$I(\lambda)$	$F(\lambda)$	$I(\lambda)$
[O II]	3727	323	512	509	808	475	754	1080	1710	940	1490
[Ne III]	3869	95	143	88	132	83	124	94	141
He I + H ζ	3889	28	41
[Ne III] + He	3968	44	63	(33)	(47)	40	58
[S II]	4071	39	54	25	34
H δ	4102	20	28
[Fe V]	4227	12	16
H γ	4340	44	56	39	49
[O III]	4363	23	30
He I	4471	14	17
[Fe III]	4658	17	19
He II	4686	55	59	(20)	(22)	27	29
H β	4861	100	100	100	100	100	100	100	100
[O III]	4959	163	157	125	120	199	191	325	312
[O III]	5007	624	588	430	405	667	628	882	831	1040	982
[Fe II] + [Fe VII]	5159	12	11
[N I]	5199	<25	<22	<10	<9
[Fe III] + [Fe III]	5270	13	11
[N II]	5755	<30	<22	<20	<15	<10	<7
He I	5876	61	42	39	28	27	19	63	44
[Fe VII]	6087	8	6
[O I]	6300	183	114	129	81	251	157
[S III]	6312	<20	<13
[O I]	6364	56	35	45	28	83	51
[N II]	6548	(360)	(212)	598	352	160	94
H α	6563	(420)	(246)	536	314	525	308	(512)	(300)	593	347
[N II]	6583	(75)	(44)	1280	747	1610	940	3230	1890	490	286
He I	6678
[S II]	6717	126	71	431	244	363	206	349	198	446	253
[S II]	6731	152	86	557	314	406	229	359	203	540	305
[Ar III]	7136	54	28	33	17
[Fe II]	7155	(35)	(18)	18	9
[O II]	7325	91	45
$f(\text{H}\beta)$ ergs cm ⁻² s ⁻¹		6.8 E-15		4.7 E-15		1.0 E-14		...		2.1 E-14	

III. RESULTS

a) Hydrogen and Helium Lines

Previous studies of the Balmer decrement for the Crab filaments have concluded that the emission lines of hydrogen result from radiative recombination with no substantial contribution from collisional excitation. Although the strength of H α at one position (region 1') was estimated to be $3.5 \times I(\text{H}\beta)$, Miller (1978) attributed the difference from the recombination value of $2.85 \times I(\text{H}\beta)$ to errors in deblending H α from the adjacent [N II] $\lambda\lambda 6583, 6548$ lines. While Davidson (1979) found a range of H α /H β ratios of 2.55 to 4.11 for the filaments, he also concluded that the H β /H γ /H δ line intensities were consistent with pure recombination values and suspected his H α values (in fact, all his line intensities redward of 6000 \AA) were overestimated by 10% to 25% due to problems in connecting his separate blue and red scans.

Because our blue and red spectral coverage was simultaneous, we avoided any uncertainties in repositioning the slit or calibrating separate red and blue scans.

Nevertheless, our determination of the intensity of H α for the filaments was limited by the blending from fainter emission systems. An inspection of Table 3 shows that the H α /H β ratio ranges from 2.5 to 3.75 with an average near 3.0. While observational and deblending errors certainly account for part of this range in values, a Balmer decrement slightly steeper than that from pure recombination is probably present in some filaments. The H α /H β value of 3.5 for position 8 (where the signal-to-noise ratio is high and deblending H α from the [N II] is not a serious problem) is in rough agreement with Davidson's value of 3.85 for this region after including an overestimate of H α by 10%. Moreover, our data for nearly the same emission filament as Miller's position 1 (our position 10), where he measured an H α /H β of 3.5, indicates a value of 3.75. Thus, some collisional excitation is probably present in at least some filaments. Because a small amount of collisional excitation mimics a small amount of reddening, slight differences in extinction between filaments is also a possibility. However, Minkowski (1942) and Baade (1942) have argued that absorption within the nebula is either small or absent based on

TABLE 3—Continued

LINE	$\lambda(\text{\AA})$	FILAMENT POSITIONS					
		8'		9		10	
		$F(\lambda)$	$I(\lambda)$	$F(\lambda)$	$I(\lambda)$	$F(\lambda)$	$I(\lambda)$
[O II]	3727	436	692	1390	2210	467	740
[Ne III]	3869	140	210	57	86
He I + H ζ	3889	58	86	35	51
[Ne III] + H	3968	62	89	33	48
[S II]	4071	24	33	59	80
H δ	4102	25	35	17	24
[Fe V]	4227	14	19
H γ	4340	50	64	40	50
[O III]	4363	10	12	12	16
He I	4471	30	36	15	18
[Fe III]	4658	(8)	(9)	16	18
He II	4686	47	51	37	40
H β	4861	100	100	100	100	100	100
[O III]	4959	437	420	230	221
[O III]	5007	638	601	1360	1280	715	675
[Fe II] + [Fe VII]	5159	(10)	(9)
[H I]	5199	(8)	(7)
[Fe II] + [Fe III]	5270	(10)	(9)
[N II]	5755
He I	5876	76	53
[Fe VII]	6087	8	6
[O I]	6300	(100)	(162)	190	119
[S III]	6312
[O I]	6364	66	41
[N II]	6548
H α	6563	(463)	(271)	(640)	(375)
[N II]	6583	1140	665	(480)	(280)
He I	6678	(39)	(22)
[S II]	6717	1080	613
[S II]	6731	1130	638
[Ar III]	7136	118	61
[Fe II]	7155	(29)	(15)
[O II]	7325	85	42
$f(\text{H}\beta)$ ergs cm $^{-2}$ s $^{-1}$		1.6 E-15		2.2 E-14		1.0 E-13	

faint star counts within and nearby the nebula and from the similarity in brightness of the filaments located on both the near and far sides.

Concerning the helium line intensities, only our positions 8 and 10 had sufficiently good signal-to-noise ratios to permit accurate measurements of the intensities of the He I lines at $\lambda 3889$, $\lambda 4471$, and $\lambda 5876$. Davidson (1979) found little deviation from the theoretical values for the helium line intensities (at $T = 14,000$ K, $I(\lambda 3889)/I(\lambda 4471)/I(\lambda 5876) = 2.7/1.0/2.5$). We, too, find the He I line ratios are very close to the predicted values; for position 8, 2.5/1.0/2.7, and for position 10, 2.8/1.0/2.9.

Several of the filaments we observed, especially those in the northern portion of the nebula, show weak He I emission compared to the majority of those observed by Woltjer (1958) and Davidson (1979). For example, although our data show a range of 17 to 77 and Davidson 20 to 195, our average $I(\lambda 5876)$ relative to $I(\text{H}\beta)$ is 37, while Davidson observed 76. Most of the filaments we observed are located in the nebula's northern region, while Davidson sampled filaments generally in the southern part. Sky subtraction errors

for the nearby sky lines of Na I at $\lambda\lambda 5890$, 5896 are unlikely in view of the correct subtraction of the much brighter night sky line of [O I] $\lambda 5577$. The implications of such relatively low He I line intensities for the helium abundance in these filaments are uncertain without detailed modeling of the type described in Paper II. Nonetheless, these filaments are of interest because real variations in the nebula's abundances provide valuable clues to the presupernova's evolution and explosion. While additional spectroscopic data of the northern filaments would be of interest, our data together with published data (Davidson 1979; Miller 1979) suggest that most of the filaments with weak helium lines lie in the nebula's northern regions.

b) Electron Temperature and Densities

Table 4 lists the filaments' temperatures and densities derived from [O III], [N II], and [S II] lines. The [O III] line temperatures inferred from the ratio of $I(\lambda 5007 + \lambda 4959)/I(\lambda 4363)$ range from 11,000 to 18,300 K for the four filaments where we could accurately measure $I(\lambda 4363)$. This [O III] temperature range is consistent with

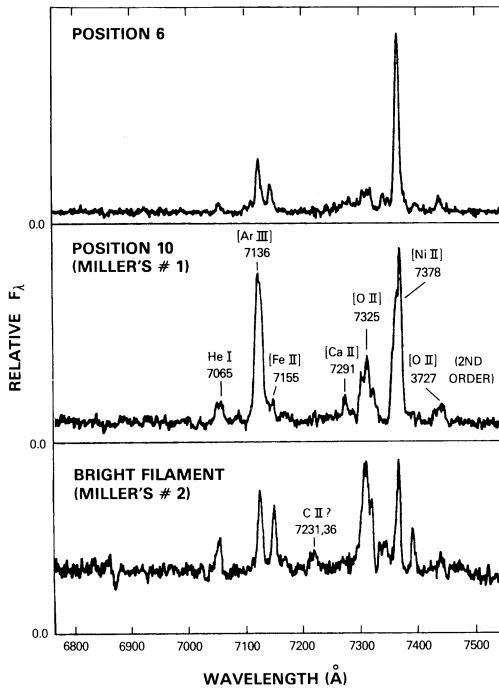


FIG. 4.—Higher dispersion scans for positions 6, 10 and a bright filament near Miller's 1978 position 2 covering the 6800–7500 Å region showing the strength of the $\lambda 7378$ feature as well as other weaker emission lines. Because of some second-order overlap, the relative fluxes shown are only approximate.

Davidson's (1979) range of 12,000 to 17,000 K as well as the two filaments observed by Miller (1978) which had temperatures of 12,000 and 16,000 K. However, some of the measured $\lambda 4363$ intensity might be due to [Fe II] at $\lambda 4359$. Faint lines of [Fe II] have been observed in some filaments (Fesen, Kirshner, and Chevalier 1978), and it is possible that weak [Fe II] $\lambda 4359$ with an intensity of $0.25 \times I(\lambda 4363)$ is present in the spectra, which would decrease our estimated [O III] temperatures by 1000 to

2500 K. The derived [O III] temperatures are much lower than observed in supernova remnants which are shock heated, yet, Contini, Kozlowsky, and Shaviv (1978) have argued that shock heating might be present in some filaments.

Upper limits for [N II] temperatures estimated from the ratio of $I(\lambda 6583 + \lambda 6548)/I(\lambda 5755)$ indicate values less than 13,600 K. For position 5 we were able to measure $\lambda 5755$ directly, and we found a value of $9,600 \pm 1500$ K. Because we estimated the electron density from the [S II] $\lambda 6717/\lambda 6731$ line ratio (see below), we could derive [O II] and [S II] temperatures using the $\lambda 7325/\lambda 3727$ and $\lambda 6725/\lambda 4071$ line ratios. The data for positions 4 and 8 indicate [O II] temperatures of 7700 and 9000 K, with a higher value of 16,500 K for position 10. A similar temperature estimate was obtained by Miller (1978) for this latter position assuming $N_e = 10^3$. Temperature estimates determined from the [S II] lines are less reliable because of possible contamination of the [S II] $\lambda \lambda 4069, 4076$ blend by emission of [Fe III] at $\lambda 4069$ and [Fe V] at $\lambda 4072$ and $\lambda 4078$ as discussed by Davidson (1978, 1979). Nevertheless, reasonably good agreement with the [O II] temperatures and [N II] upper limits are obtained for the regions 6, 8, and 10 yielding $T = 7000$ –8000 K, with a higher value of 13,000 K for position 5.

Electron density estimates listed in Table 4 were inferred from the observed ratios of [S II] $\lambda 6717/\lambda 6731$, using the S^+ atomic parameters of Pradhan (1978). The average filament density is near 1300 cm^{-3} , with individual values ranging from 550 cm^{-3} to 3000 cm^{-3} . This is consistent with the densities estimated by Osterbrock (1957), Woltjer (1958), and Davidson (1978, 1979). At position 4 we also measured the density sensitive [O II] $\lambda 3729/\lambda 3726$ line ratio which gave a value of 0.75 indicating a density of $2000 \pm 400 \text{ cm}^{-3}$, in reasonable agreement with the $1600 \pm 500 \text{ cm}^{-3}$ implied by the [S II] lines. Slightly different locations and/or density variations within the bright condensation at position 8 probably account for the difference in estimated electron density between our high and low dispersion scans. The

TABLE 4
ELECTRON TEMPERATURES AND DENSITIES

POSITION	TEMPERATURES (K)				DENSITIES (cm^{-3}) [S II]
	[O III]	[N II]	[O II]	[S II]	
1	$14,000 \pm 2000$	$< 13,200$	1400 ± 500
2	550 ± 350
3	1150 ± 550
4	$< 11,800$	7700 ± 2500	...	1600 ± 500
5	$< 21,500$	9600 ± 1500	...	$13,000 \pm 2000$	625 ± 400
5'	1350 ± 500
6	$< 13,600$...	8500 ± 1500	1700 ± 550
7	$< 10,000$	1100 ± 400
7'	800 ± 400
8	$18,300 \pm 2500$	$< 12,100$	9000 ± 3000	7000 ± 1500	1400 ± 500^a
9	$11,000 \pm 2000$
10	$16,000 \pm 2500$...	$16,000 \pm 3500$	7500 ± 1500	850 ± 400

^a A high-dispersion scan indicated $N_e \sim 3500 \text{ cm}^{-3}$.

high dispersion data indicate that in fact the main emission feature observed at position 8 is really composed of at least two separate components having a radial velocity difference of about 200 km s^{-1} . At low dispersion the [S II] ratio gives a density estimate of $1400 \pm 500 \text{ cm}^{-3}$, while a high dispersion scan taken on a different night indicates a higher density close to $3000 \pm 400 \text{ cm}^{-3}$. This region was observed by Davidson who reported a high density of $3200 \pm 1000 \text{ cm}^{-3}$.

c) Faint Emission-Line Identifications

Table 3 lists the line intensities for some weak emission lines in the Crab's spectra. These include [Fe V] $\lambda 4227$, [Fe II] $\lambda 5159$ (possibly blended with [Fe VII] $\lambda 5159$), [N I] $\lambda 5199$, the [Fe II] and [Fe III] blend at $\lambda 5270$, [Fe VII] $\lambda 6087$, [Ar III] $\lambda 7136$, [Fe II] $\lambda 7155$ and some upper limits for [S III] $\lambda 6312$. Other faint lines not included in Table 3 but present in the data are [Fe VII] $\lambda 5712$ in position 8, and He I $\lambda 4026$ at position 9, and we note the possible presence of C II at 7231 \AA and 7236 \AA in the data for the bright filament near Miller's position 2. Davidson (1979) has reported the possible detection of C II $\lambda 4267$ emission near our position 9, but we could not confirm this from our data. The detection of [Fe II] at $\lambda 5159$ and $\lambda 7155$ establishes the presence of [Fe II] lines in Crab filament spectra as suspected by Davidson and Humphreys (1976) and Fesen, Kirshner, and Chevalier (1978). The wide range of ionization species of iron (Fe^+ , Fe^{2+} , Fe^{4+} , and Fe^{6+}) seen in position 8 suggests a stratified line emitting region in this filament. An estimate for the electron temperature in the [Fe VII] line emitting region would be of some interest and could be obtained by measuring the relative strengths of both the [Fe VII] $\lambda 6087$ and $\lambda 3760$ lines from a single filament (see Nussbaumer and Osterbrock 1970).

The identification of a moderately strong feature at $7378 \pm 1 \text{ \AA}$ is interesting. It was first detected in the spectrum of the Crab by Miller (1978) who reported an intensity comparable to the [O II] $\lambda 7325$ blend. Our red spectra for positions 6, 10, and the bright filament near Miller's position 2 show the feature has a flux about 10%–20% that of $\text{H}\alpha$. This emission line has been seen in other SNRs (see Fesen and Kirshner 1980) as well as in H II regions (Grandi 1975; Thackeray 1975) and Herbig-Haro objects (Dopita 1978) and is usually identified as [Ni II] at 7377.9 \AA . Atomic data by Garstang (1958) as well as observations of the Orion Nebula and η Carinae indicate that a second [Ni II] line from the same multiplet at 7411.3 \AA should also be seen at about half the strength of the 7378 \AA line. While a feature having such an intensity can be ruled out from the data shown in Figure 4, in the spectrum for position 6 where the $\lambda 7378$ feature is especially strong, there may be a weak emission near 7411 \AA with about 5%–10% the intensity of the $\lambda 7378$ line. Recent atomic calculations by Nussbaumer and Storey (1982) show that temperature and density can have significant effects on the $\lambda 7378/\lambda 7411$ ratio and that the observed line ratio is consistent with the physical conditions derived by other means for the Crab's filaments.

IV. DISCUSSION

These new data together with those previously obtained by Osterbrock (1957), Woltjer (1958), Miller (1978), and Davidson (1978, 1979), permit reliable estimates of some of the filaments' physical parameters. From nearly 30 [O II] and [S II] ratio measurements on almost two dozen separate filaments, the average electron density is around 1300 cm^{-3} . Although the total range in density is 500 to 4000 cm^{-3} , all but three filaments exhibit densities between 500 and 2000 cm^{-3} . However, these measurements are biased toward the brighter filaments. The density of fainter and possibly less dense filaments is still relatively unknown but could be measured using the [O II] lines. In the highly ionized and faint outer filaments observed by Davidson (1978), the [S II] lines were often very weak while there was still substantial [O II] emission.

Using 16 recent spectrophotometric measurements on 11 filaments, the [O III] electron temperatures lie between 11,000 and 18,000 K and average around 15,000 K. Woltjer's photographic data are generally consistent with these results but suggest a wider range of [O III] temperatures. For the most part, a filament's [O II], [N II], and [S II] temperatures are considerably lower than its [O III] temperature, but there are possible exceptions (e.g., position 10).

As noted by previous authors, the relative intensities of many forbidden lines vary considerably over the nebula. The photographic data of Woltjer and Trimble have suggested that the ratio of [O III]/[O II] varies systematically as a function of distance from the nebula's center. While only a few of the filaments studied photometrically have measured nebula radial distances (cf. Trimble 1968), our data are consistent with such a [O III]/[O II] gradient. While Kirshner (1974) observed for the whole nebula an [O III]/ $\text{H}\beta$ ratio of 15, there appears to be a rather large range of values present throughout the filaments; from about 3 to nearly 45. The [N II] lines also exhibit a considerable spread in emission line strengths, with $\lambda 6583/\text{H}\beta$ varying from 0.44 to nearly 19. Minkowski (1942) and Chevalier and Gull (1975) reported that strong [O I] emission is usually accompanied by strong [S II] emission; we find a good correlation between [O I] and [S II] line strength for those filaments exhibiting $I(\lambda 6717 + \lambda 6731)$ smaller than 700. Also, the [O I] line strengths do not appear to be strongly correlated with filament density.

Although the chemical composition of the nebula's filaments is best treated through detailed modeling of the data (see Paper II), the factor of nearly 10 change in He I $\lambda 4471$, 5876 recombination line strengths suggests some helium abundance differences among the filaments. In other emission nebulae (whether photoionized or collisionally ionized), [N II]/ $\text{H}\alpha$ ratios of 3 or more are usually taken as indicating a nitrogen enrichment. While this may not necessarily be the case in the Crab (because of the character of the input spectrum and effects of the high helium abundance), nitrogen abundance variations among filaments might be partially responsible for some

of the observed spread in [N II] line intensities. The strength of the forbidden iron lines does not suggest any peculiar abundance of iron. This is suggested by the intensity of the [Fe VII] $\lambda 6078$ reported here for position 8 which, when combined with Davidson's (1979) [Ne V] $\lambda 3426$ measurement and following Nussbaumer and Osterbrock's (1970) discussion, suggests a near normal Fe/Ne abundance ratio of 0.17.

We would like to thank Kris Davidson for useful

discussions, Eliot Malumuth for obtaining some of the high dispersion red data, and Chris Price, Fred Feldman, and Alan Koski for providing the software for the data reduction and Harry Nussbaumer for providing a preprint of his [Ni II] work with Peter Storey. Support was provided in part by NSF grants AST 77-17600 and AST 81-5050 and the University of Michigan Astronomy Department's Lawton Fellowship. This work was done in partial fulfillment of R. A. F.'s doctoral dissertation requirements at the University of Michigan.

REFERENCES

- Baade, W. 1942, *Ap. J.*, **96**, 188.
 Chevalier, R. A., and Gull, T. R. 1975, *Ap. J.*, **200**, 399.
 Contini, M., Kozlowsky, B. Z., and Shaviv, G. 1978, *Astr. Ap.*, **68**, 443.
 Davidson, K. 1978, *Ap. J.*, **220**, 177.
 ———. 1979, *Ap. J.*, **228**, 179.
 Davidson, K., Crane, P., and Chincarini, G. 1974, *A.J.*, **79**, 791.
 Davidson, K., and Humphries, R. M. 1976, *Pub. A.S.P.*, **88**, 312.
 Dopita, M. A. 1978, *Ap. J. Suppl.*, **37**, 117.
 Fesen, R. A., and Kirshner, R. P. 1980, *Ap. J.*, **242**, 1023.
 Fesen, R. A., Kirshner, R. P., and Chevalier, R. A. 1978, *Pub. A.S.P.*, **90**, 32.
 Garstang, R. H. 1958, *M.N.R.A.S.*, **118**, 234.
 Grandi, S. 1975, *Ap. J. (Letters)*, **199**, L43.
 Henry, R. C., and MacAlpine, G. M. 1982, *Ap. J.*, **258**, 11 (Paper II).
 Kirshner, R. P. 1974, *Ap. J.*, **194**, 323.
 Miller, J. S. 1973, *Ap. J. (Letters)*, **180**, L83.
 Miller, J. S. 1974, *Sci. Am.*, **231**, 34.
 ———. 1978, *Ap. J.*, **220**, 490.
 Minkowski, R. 1942, *Ap. J.*, **96**, 199.
 Munch, G. 1958, *Rev. Mod. Phys.*, **30**, 1042.
 Nussbaumer, H., and Osterbrock, D. E. 1970, *Ap. J.*, **161**, 811.
 Nussbaumer, H., and Storey, P. J. 1982, preprint.
 Oke, J. B. 1974, *Ap. J. Suppl.*, **27**, 21.
 Osterbrock, D. E. 1957, *Pub. A.S.P.*, **69**, 227.
 Pradhan, A. K. 1978, *M.N.R.A.S.*, **183**, 89P.
 Stone, R. D. S. 1977, *Ap. J.*, **218**, 767.
 Thackeray, A. D. 1975, *M.N.R.A.S.*, **173**, 49P.
 Trimble, V. 1968, *A.J.*, **73**, 535.
 ———. 1970, *A.J.*, **75**, 926.
 Woltjer, L. 1958, *Bull. Astr. Inst. Netherlands*, **14**, 39.
 Wu, C-C. 1981, *Ap. J.*, **245**, 581.

ROBERT A. FESEN: NASA/Goddard Space Flight Center, Code 683, Laboratory for Astronomy and Solar Physics, Greenbelt, MD 20771

ROBERT P. KIRSHNER: Department of Astronomy, University of Michigan, Ann Arbor, MI 48109